International Journal of
AI ELECTRICAL CIVIL AND MECHANICAL ENGINEERING
Peer Reviewed, Referred & Indexed Journal
ISSN: 3070-0434 www.zesterapublications.com Original Research Paper

AN AIRCRAFT PROPELLER BLADE MODELED AND ANALYZED USING CATIA V5 WITH ANSYS CFX FOR COMPUTATIONAL FLOW

T. THOMAS ALWA EDISON[1], Dr. B. SANDHYA RANI[2]
[1]PG Student, CAD/CAM, Ellenki College of Engineering and Technology.
[2]Assistant Prof. & Head of the Dept., Department of Mechanical Engineering, Ellenki College of Engineering and Technology.

Abstract - Aircraft propellers are among the most demanding rotating aero-structural components because to the simultaneous application of centrifugal loads, aerodynamic bending and torsional stresses, and vibratory stimulation. Compared to their fiber-reinforced composite counterparts, traditional aluminum blades are both heavier and more prone to fatigue, despite their ease of production. An airplane propeller with several blades, designed for fabrication in a fiber-reinforced polymer composite, is detailed in this work along with its computational flow analysis and three-dimensional solid modeling. A twisted aerofoil blade profile, a central hub, and the whole eight-blade rotor assembly were created by modeling the geometry in CATIA V5 utilizing the Part Design, Wireframe and Surface Design, and Assembly Design workbenches. Importing the CATIA assembly into ANSYS Workbench allowed us to examine the flow field around the spinning propeller on an unstructured tetrahedral mesh with 7,960 nodes and 41,116 elements using the Fluid Flow (CFX) system. Within 47 iterations of the outer loop, a steady-state laminar-flow solution with a uniform input velocity of 64 m/s converged to an RMS residual goal of 1×10^{-4}, with normalized imbalances for the mass and momentum equations within ±0.04%.

The rotor's thrust-generation mechanism was confirmed by post-processing, which showed pressure differentials throughout the blade surfaces ranging from around -3.27 MPa to +6.95 MPa and local flow velocities approaching 115 m/s at the tips of the blades. Along with the geometric design, the report includes the pressure, viscous forces, and moments that were retrieved from the solver and applied to the blade and hub surfaces. This provides a verified baseline flow field that may be used for future mapping onto a structural/composite laminate model of the blade. In order to advance a design to the detailed engineering stage, it must undergo specific refinements, such as turbulence modeling, rotating-reference-frame analysis, and one-way fluid-structure interaction (FSI) onto a composite lay-up. This study proves that an integrated CATIA-to-ANSYS workflow is appropriate for the preliminary aero-structural design evaluation of composite aircraft propeller blades.

Important Terms - Composite blades, aircraft propellers, CATIA V5, ANSYS CFX, CFD, aerodynamic analysis, solid modeling, rotor design, and computational fluid dynamics.

I. INTRODUCTION

Aeroplanes that use propellers to propel themselves forward create thrust by spinning aerodynamically constructed blades, which, according to Newton's third law, causes an equal and opposite reaction force to be generated in the forward direction [1, 2]. By varying the twist, chord, and thickness of the blades along their span, we can achieve optimal angle of attack for every section, just as if the blades were rotating wings whose local relative airflow were the vector sum of the tangential and axial velocities [2], [18]. Blades for propellers have evolved through many materials, including laminated hardwood, forged aluminum alloy, and now fiber-reinforced polymer (FRP) composites. In contrast to aluminum blades, which are bulkier, more fatigue-and corrosion-prone, and less corrosion-resistant, epoxy laminates reinforced with carbon and glass fibers provide a high specific stiffness-to-weight ratio, adjustable anisotropic characteristics, longer fatigue life, and resistance to corrosion [4-6]. Composite blades enable weight reduction and structural optimization at the same time due to the loading direction-tunable fiber orientation and stacking sequence of composite laminates. This, in turn, improves fuel efficiency, range, and climb performance by reducing gyroscopic loads, hub, and bearing loads. Aerodynamics, structural mechanics, materials science, and manufacturing are all involved in the design of composite propeller blades. First, the aerodynamic performance criteria are established.

Then, parametric CAD geometry is generated. Then, computational fluid dynamics (CFD) analysis is carried out to determine the pressure loading. Finally, a composite finite-element structural model is used to map this loading. The initial two steps of this process are covered in this work: (i) using CATIA V5 for parametric solid modeling of an eight-blade composite propeller/rotor and (ii) using ANSYS CFX for steady-state computational fluid dynamics (CFD) of the surrounding flow field. This process yields a validated

Received: 20-06-2026 | Accepted: 25-07-2026 | Published: 31-07-2026

International Journal of
AI ELECTRICAL CIVIL AND MECHANICAL ENGINEERING
Peer Reviewed, Referred & Indexed Journal
ISSN: 3070-0434 www.zesterapublications.com Original Research Paper

pressure and velocity field as well as integrated force/moment data that can be used as loading input for a future structural analysis of composite laminates.

A. Inspiration and Goals

Compared to aluminum, composite blades are more resistant to fatigue and corrosion. Before designing the structural details, parametric CAD modeling in CATIA enables quick iterations of the blade shape (chord, twist, aerofoil). Cutting down on time and money spent on physical prototypes and wind tunnel testing is possible with an integrated CATIA-ANSYS digital process. Consequently, this work aims to: (1) examine the structural and aerodynamic design considerations for a composite propeller blade for an aircraft; (2) use CATIA V5 to create a parametric three-dimensional CAD model of the blade, hub, and rotor assembly; (3) study the assembly using ANSYS CFX for computational fluid dynamics (CFD); and (4) report the results as a pressure field, velocity field, and integrated forces/moments to use as a loading basis for the composite structural design that follows.

B. Extent and Restrictions

A comprehensive investigation of the composite laminate structure, including ply-by-ply stress, deflection, and modal behavior, is planned for future work; the current effort focuses on computer-aided design (CAD) geometric design and computational fluid dynamics (CFD) flow. To establish and validate the CFD workflow, the analysis was run as a steady-state, laminar, single-phase simulation with water as the working fluid and the propeller in a stationary (non-rotating) reference frame. However, the mesh, boundary conditions, and solution methodology can be easily transferred to an air-medium, rotating-frame simulation that represents real flight conditions.

II. REVIEW OF LITERATURE

By considering the various radial blade sections as separate two-dimensional aerofoils and including the corresponding elemental lift and drag forces throughout the span, Blade Element Theory (BET) was one of the first analytical methods to estimate propeller performance [1, 3]. Although BET is still helpful for conceptual design and doesn't cost much to compute, it doesn't take into account three-dimensional effects like radial flow or interactions between neighboring parts. One of the most popular tools for propeller, rotor, and wind turbine design is Blade Element Momentum Theory (BEMT), which is the result of combining BET with actuator-disc Momentum Theory. BEMT couples blade loading with induced-velocity prediction and is still used today [2, 3], though it still uses idealized aerofoil data and empirical corrections. Since computational advancements have allowed CFD to directly solve the governing Navier-Stokes equations, it has become an essential tool for propeller aerodynamic study, resolving three-dimensional effects that BET/BEMT are unable to capture. CFD study of propellers, axial fans, and turbomachinery rotors is often performed using ANSYS Workbench, which combines DesignModeler/SpaceClaim geometry clean-up, ANSYS Meshing, and either the Fluent or CFX solver [7]-[10]. For rotating machinery, the CFX coupled algebraic multigrid solver works fine with frozen-rotor and transient rotor-stator interface models. However, before running a full rotating-frame simulation, it is common practice to conduct a stationary-frame steady analysis with a specified inlet velocity to check the quality of the mesh, the solver's convergence, and the boundary conditions. Anisotropic laminate theory and finite-element analysis have been used to examine the structural aspects of composite propeller blade design, namely the ply-level stresses, deflection, and modal behavior under aerodynamic loading [4]-[6], [15], [16]. In a related study, the pressure loads for wind turbine and propeller blades were combined with FEA structural models [17]. On the other hand, there is a dearth of scholarly work that details a unified and repeatable process from CATIA to ANSYS, beginning with parametric blade geometry and ending with convergent flow-field findings. This workflow is specifically designed to feed into a later composite structural study. To fill this need, this study documents the whole approach using a real CFX problem that has been addressed.

III. STUDY DESIGN

Methodology adheres to a sequential digital design-and-analysis workflow, beginning with design requirements formulation and ending with post-processing of the converged flow field. The workflow includes parametric CAD modeling in CATIA V5, enclosure of the model in a fluid domain, mesh creation in ANSYS CFX, and CFD solution in ANSYS.

A. Technical Details

Rotor design specifications (table 1)

Received: 20-06-2026 | Accepted: 25-07-2026 | Published: 31-07-2026

International Journal of
AI ELECTRICAL CIVIL AND MECHANICAL ENGINEERING
Peer Reviewed, Referred & Indexed Journal
ISSN: 3070-0434 www.zesterapublications.com Original Research Paper

Parameter	Value / Description
Number of blades	8
Overall rotor diameter	0.44 m – 0.67 m (fluid-domain envelope)
Hub type	Conical/spherical central boss
Blade profile	Twisted, curved aerofoil-type blade
Modelling software	CATIA V5 (Part Design, Assembly Design)
CFD software	ANSYS Workbench 19.5 – Fluid Flow (CFX)

Table II shows that the main candidate laminate for the composite blade construction is unidirectional and woven carbon-fiber-reinforced epoxy (CFRP), which has a high specific stiffness and fatigue resistance. A less expensive alternative is glass-fiber-reinforced epoxy (GFRP), and aluminum alloy is kept as an isotropic baseline for comparison.

The second table compares the candidates' materials.

Material	Remarks
CFRP (epoxy)	Highest specific stiffness/strength; excellent fatigue life; higher cost
GFRP (epoxy)	Good strength, lower cost, higher density than CFRP
Aluminium alloy (baseline)	Isotropic, established manufacturing, heavier, lower fatigue life

B. CATIA V5: Simulation of Solids

The aerofoil section of the blade and the distribution of radial twist and chord were established by drawing sections at regular intervals along parallel reference planes, which were then rotated around the root axis of the blade to include the spanwise twist. Utilizing the Multi-section Solid function in the Part Design workbench, these segments were elevated into a unified three-dimensional blade solid. To alleviate stress concentration, fillets were placed at the blade root to ease the transition into the hub. A solid of rotation (Shaft feature) around the rotor axis was utilized to simulate the central hub. Then, the eight-blade rotor was created by arraying the blade solid around the hub at equal angular spacing using a Circular Pattern. The Assembly Design workbench was used to integrate the separate elements according to the Coincidence, Concentricity, and Offset requirements (Fig. 1).

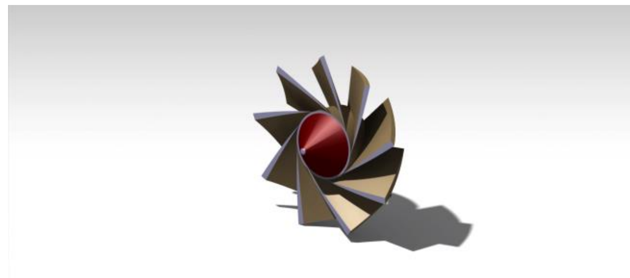

Fig. 1. This is an isometric image of the finished CATIA V5 composite propeller/rotor assembly with eight blades.

C. Domain, Mesh, and Solver Configuration for CFD

An external fluid domain, which represents the volume around the rotor, was used to load the completed CATIA assembly into ANSYS Workbench 19.5. The blade/hub surfaces, outside duct wall, input, and exit were all designated with names. To accommodate the twisting and curved surfaces of the blades, the fluid domain was discretized using an unstructured all-tetrahedral mesh with 7,960 nodes and 41,116 elements (Table III).

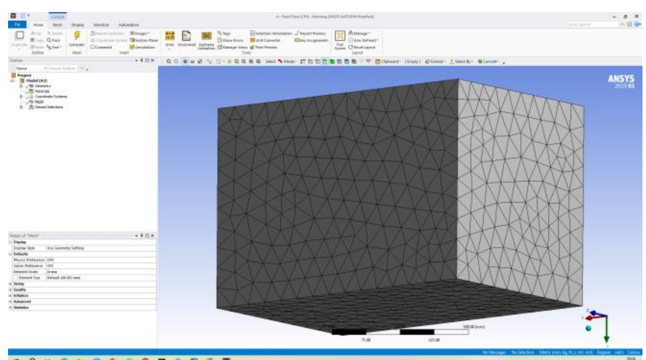

Fig. 2. Volume and surface mesh of a tetrahedron formed on the fluid domain around the propeller.

The table MESH DATA PART III

International Journal of
AI ELECTRICAL CIVIL AND MECHANICAL ENGINEERING
Peer Reviewed, Referred & Indexed Journal
ISSN: 3070-0434 www.zesterapublications.com Original Research Paper

Mesh Statistic	Value
Total nodes	7,960
Total elements	41,116 (100% tetrahedral)
Total faces	4,340
Min. orthogonal angle	40.2° (acceptable)
Max. expansion factor	204 (isolated cells, ~1% of mesh)
Max. aspect ratio	10 (within acceptable limit)
Domain extent	0.445 m – 0.671 m

The mesh, boundary conditions, and solver methodology can be easily applied to a simulation with air as a medium, with a rotating reference frame. The working fluid for this preliminary validation case was water, with a density of 1000 kg/m³ and a dynamic viscosity of 0.891×10^{-3} Pa·s, in a stationary reference frame under isothermal, non-buoyant, laminar-flow assumptions. Table IV shows that the following conditions were applied: a uniform normal-speed inlet of 64 m/s, an average-static-pressure outlet of 0 Pa relative with a blend factor of 0.05, and no-slip conditions on all surfaces of the wall and blade/hub. The model also features a High-Resolution advection scheme, Auto Timescale control, and an RMS residual convergence target of 1×10^{-4}, achieved using a double-precision solver.

Table IV: Conditions at the Boundary

Boundary	Condition
Inlet	Normal speed = 64 m/s
Outlet	Average static pressure = 0 Pa (rel.)
Duct/enclosure wall	No-slip
Blade & hub surfaces	No-slip

IV. SUMMARIES AND ANALYZES

A. Bringing Things Together

The linked U-, V-, W-, and P-Mass equations converged to the root-mean-square (RMS) goal of 1×10^{-4} in around 18.5 seconds of wall-clock solver time, after 47 iterations in the outer loop. A numerically converged and mass/momentum conservative solution was confirmed by normalized imbalances at convergence of −0.0381% (U-momentum), 0.0002% (V-momentum), −0.0016% (W-momentum), and 0.0002% (P-mass), all of which were well within the universally recognized ±1% engineering convergence limit. The existence of a fully turbulent flow was confirmed by the solver's output, which indicated an effective Reynolds number of about 3.62×10^{7}. In order to validate the meshing and boundary-condition workflow, the laminar assumption was maintained. A necessary refinement was the identification of an appropriate turbulence closure, such as k-ω SST.

B. Distributed Pressure

Over the fluid domain, the static pressure of the convergent solution ranges from around -3.27 MPa to +6.95 MPa, as shown in Table V. According to the pressure-differential mechanism that propeller blades use to produce thrust, there is a clearly defined high-pressure area on the pressure side of the blades, concentrated around the mid-span to outer region where the relative velocities of the fluid and blade surface are highest (Fig. 3), and lower-pressure areas near the blade tips and on the suction side.

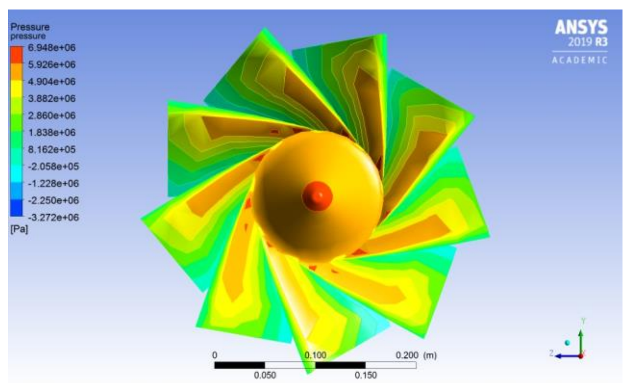

Fig. 3. Observed here is the static pressure contour on the hub and blade surfaces of the propeller.

Table V. Summary of Variable Range

Variable	Min / Max
Velocity, u-component	−112 / 63.6 m/s
Velocity, v-component	−99.7 / 96.2 m/s
Velocity, w-component	−92.8 / 99.5 m/s
Static pressure	−3.27 / 6.95 MPa
Streamline velocity magnitude	0.44 / 114.9 m/s

C. Simplifying Speed

The smooth and mostly attached flow approaching the rotor is shown by velocity streamlines traced from the inlet to the outlet (Fig. 4). As the fluid passes through and around the

International Journal of
AI ELECTRICAL CIVIL AND MECHANICAL ENGINEERING
Peer Reviewed, Referred & Indexed Journal
ISSN: 3070-0434 www.zesterapublications.com Original Research Paper

blades, it experiences acceleration and swirl, which are hallmarks of a propeller imparting axial momentum to the working fluid. Some flow separation and recirculation is seen immediately downstream of the hub in the near-wake area, and there is locally accelerated flow of up to around 115 m/s at the blade tips and in the blade-to-blade passageways.

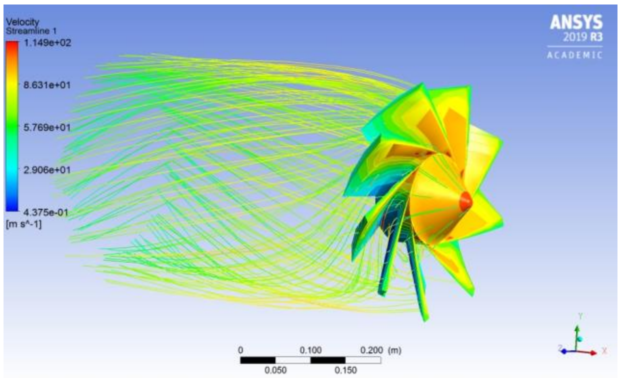

Fig. 4. The magnitude of the speed determines the color of the streamlines as they pass through the propeller.

D. Power and Time

With respect to the blade, hub, and wall surfaces, Table VI summarizes the pressure and viscous force/moment components. The aero-structural response of the blade is governed by pressure-driven loading, as the dominant load along the rotor (X) axis is a pressure force that is several orders of magnitude larger than the corresponding viscous force. The moment components are also dominated by the pressure moment about the X-axis. A composite laminate finite-element model of the blade is used to map the aerodynamic input for a subsequent one-way fluid-structure interaction (FSI). These integrated loads are a representation of those loads.

Outcome table: forces and moments that follow

Quantity (Component)	Domain Total
Pressure force, X	-4.070×10^{5} N
Pressure force, Y	8.341×10^{2} N
Pressure force, Z	2.512×10^{3} N
Viscous force, X	-4.051 N
Pressure moment, X	-2.354×10^{4} N·m
Pressure moment, Y	2.065×10^{3} N·m
Pressure moment, Z	1.032×10^{3} N·m
Viscous moment, X	8.950×10^{-2} N·m

V. Final Thoughts and Prospects

A full-fledged CATIA V5 model of an eight-blade composite propeller for an aircraft was created and built. The model includes a central hub and twisted aerofoil blade profiles. An unstructured tetrahedral mesh with 7,960 nodes and 41,116 elements with satisfactory orthogonal-angle and aspect-ratio quality was discretized from the geometry in ANSYS Workbench. All normalized equation imbalances were below 0.04%, and after 47 iterations, a steady-state CFX simulation converged to an RMS residual of 1×10^{-4}. The pressure differentials and local velocities observed in the resultant flow field ranged from around -3.27 MPa to +6.95 MPa, which is in line with the thrust-generating mechanism of a propeller in motion. The loading was mainly caused by the pressure force and moment along the rotor axis, which provided a quantified aerodynamic load case for the design of composite structures. Future work should: (i) repeat the CFX simulation with an appropriate turbulence model (e.g., k–ω SST) in place of the laminar assumption; (ii) re-define the working fluid as air at the relevant flight altitude and re-run the analysis in a Rotating Reference Frame at the design RPM; (iii) perform a mesh-independence study, particularly near the blade tip and hub fillet; (iv) map the CFX pressure loads onto a composite laminate finite-element model in ANSYS Composite PrepPost/ANSYS Mechanical to evaluate ply-level stresses, tip deflection, buckling margin and natural frequencies; (v) extend the study across a range of advance ratios to generate thrust and torque performance curves and validate against wind-tunnel or manufacturer data; and (vi) investigate the effect of ply orientation and s

A CREDENTIAL

[Guide Name] and the Mechanical Engineering Department at [Institute Name] provided invaluable assistance and direction to the author(s) over the course of this project.

REFERENCES

[1] H. Glauert, "Airplane Propellers," in Aerodynamic Theory, vol. IV, Division L, Berlin, Germany: Springer, 1935.

[2] B. W. McCormick, Aerodynamics, Aeronautics, and Flight Mechanics, 2nd ed. New York, NY, USA: John Wiley & Sons, 1995.

[3] O. Gur and A. Rosen, "Comparison between blade-element models of propellers," Aeronaut. J., vol. 112, no. 1138, pp. 689–704, 2008.

[4] J. W. Gerdes, "Composite propeller blade design and structural analysis," J. Aircraft, vol. 30, no. 4, 1993.

Received: 20-06-2026 | Accepted: 25-07-2026 | Published: 31-07-2026

International Journal of
AI ELECTRICAL CIVIL AND MECHANICAL ENGINEERING
Peer Reviewed, Referred & Indexed Journal
ISSN: 3070-0434 www.zesterapublications.com Original Research Paper

[5] A. K. Kaw, Mechanics of Composite Materials, 2nd ed. Boca Raton, FL, USA: CRC Press, 2006.

[6] R. M. Jones, Mechanics of Composite Materials, 2nd ed. Philadelphia, PA, USA: Taylor & Francis, 1999.

[7] ANSYS Inc., ANSYS CFX-Solver Theory Guide, Release 19.5. Canonsburg, PA, USA: ANSYS Inc., 2019.

[8] ANSYS Inc., ANSYS CFX-Solver Modeling Guide, Release 19.5. Canonsburg, PA, USA: ANSYS Inc., 2019.

[9] ANSYS Inc., ANSYS Meshing User's Guide, Release 19.5. Canonsburg, PA, USA: ANSYS Inc., 2019.

[10] H. K. Versteeg and W. Malalasekera, An Introduction to Computational Fluid Dynamics: The Finite Volume Method, 2nd ed. Harlow, U.K.: Pearson Education, 2007.

[11] Dassault Systèmes, CATIA V5 Part Design User's Guide. Vélizy-Villacoublay, France: Dassault Systèmes.

[12] Dassault Systèmes, CATIA V5 Assembly Design User's Guide. Vélizy-Villacoublay, France: Dassault Systèmes.

[13] M. H. Sadraey, Aircraft Design: A Systems Engineering Approach. Chichester, U.K.: John Wiley & Sons, 2013.

[14] R. K. Bansal, Fluid Mechanics and Hydraulic Machines, 9th ed. New Delhi, India: Laxmi Publications, 2010.

[15] R. Hoskins and M. Kingham, "Design and analysis of a composite propeller blade for a light aircraft," Proc. Inst. Mech. Eng., Part G: J. Aerosp. Eng., 2015.

[16] S. S. Ochs, T. S. R. Reddy, S. N. Patnaik, and D. A. Hopkins, "Composite propeller analysis," NASA Tech. Memo., NASA Glenn Research Center, Cleveland, OH, USA, 2001.

[17] S. Rajendran and C. V. Narasimha Rao, "Structural and aerodynamic analysis of a wind turbine/propeller blade using CFD-FEA coupling," Int. J. Eng. Res. Technol., vol. 4, no. 6, 2015.

[18] J. D. Anderson, Fundamentals of Aerodynamics, 6th ed. New York, NY, USA: McGraw-Hill Education, 2017.

Received: 20-06-2026 | Accepted: 25-07-2026 | Published: 31-07-2026